ELSEVIER

Journal of Chromatography A, 835 (1999) 3–18

JOURNAL OF CHROMATOGRAPHY A

Influence of solvent uptake and swelling by poly(styrene–divinylbenzene) column packings on sample sorption rate and band broadening in reversed-phase liquid chromatography

Barbara Ells, Ying Wang, Frederick F. Cantwell*

Department of Chemistry, University of Alberta, Edmonton, Alberta, Canada T6G 2G2

Received 7 October 1998; received in revised form 15 December 1998; accepted 15 December 1998

Abstract

Porous poly(styrene–divinylbenzene) (PS–DVB) HPLC packings give broad, tailed peaks for some types of solutes. This phenomenon is due to sorption of these solutes into the polymer matrix where they experience very slow, hindered diffusion. It is known that the presence of small amounts of tetrahydrofuran (THF) in the methanol (MeOH)–H_2O mobile phase yields narrower and less tailed peaks for such solutes. In this study, Hamilton PRP-∞, a nonporous PS–DVB polymer, serves as a model for the matrix of porous polymers. The following measurements were made: sorption isotherms for MeOH and THF from aqueous solution; swelling of PRP-∞ as a function of activity of MeOH and THF in aqueous solution; and both sorption isotherms and sorption rate curves for the solute naphthalene from various solvent mixtures. The addition of 2% THF to 70:30 MeOH–H_2O produced an additional 0.4% swelling, an 11% decrease in the sorption capacity and a 90% increase in the diffusion coefficient of naphthalene in PRP-∞. The increase in the diffusion coefficient, which is responsible for the improved elution peak shape of naphthalene, is shown to be caused by the decrease in sorption capacity, rather than by the additional swelling. The sorbed THF serves to fill and ''block'' the smallest, most highly hindered micropores in the polymer matrix.

Keywords: Solvent uptake; Swelling; Band broadening; Sorption rate; Sorption isotherms; Tetrahydrofuran

1. Introduction

Poly(styrene–divinylbenzene) (PS–DVB) copolymers act as sorbents in reversed-phase liquid chromatography (RPLC). Usually it is porous PS–DVB packings that are employed because they provide a large surface area. The macroporous structure of these porous polymers has been characterized [1] and their properties as sorbents have been reviewed [2–5]. Commercially available porous PS–DVB packings include Amberlite XAD-2 [6,7], PLRP-S [2], PRP-1 [8,9], and others [3].

While PS–DVB packings have the advantages of both chemical stability at high and low pH and the absence of residual silanol groups, they suffer from the disadvantage of yielding lower chromatographic efficiencies than silica-based octadecylsilyl bonded-phase packings of the same particle size. The lower column efficiency is due to a slow intraparticle sorption rate. Specifically, it is due to slow diffusion of solute molecules within the polymer matrix [3,5,10–16].

Sample compounds that have solubility parameters

*Corresponding author.

0021-9673/99/$ – see front matter
PII: S0021-9673(98)01070-X

comparable to that of PS–DVB (i.e. δ=18.6–19.0 $(MPa)^{1/2}$) [13,17] have a greater propensity to diffuse into the polymer matrix than do those with very different δ. Structural features of the sample compound such as planarity and rigidity also influence this tendency [11,13]. Sorption of sample compounds into the polymer matrix, when it occurs, is assumed to take place in addition to the usual process of adsorption onto the walls of larger pores [11,16,18].

It is known that the composition of the aqueous–organic mobile phase can have a significant effect on the extent to which excessive band broadening and tailing occur [2,12,13,19–21]. For the three commonly used organic modifiers, the tail-suppressing effect increases in the order: methanol (MeOH)< acetonitrile (AN)<tetrahydrofuran (THF), for which the solubility parameters are 29.7, 24.7, and 18.6 $(MPa)^{1/2}$, respectively [11,22,23]. For comparison, δ=47.9 for water [11] which is a nonsorbed solvent in RPLC. The presence, in a ternary solvent mixture, of even a small amount of an organic solvent with δ near that of PS–DVB, such as 5% THF in MeOH–water, can significantly improve sample peak shape [12]. It has generally been inferred that it is solvent-induced swelling of the polymer matrix by sorbed THF that is responsible for decreases in sample peak bandwidth and tailing, because diffusion of the sample compound is less hindered in the swollen polymer [12,13,19–21]. In addition, ''selective binding'' of THF by micropores, which would otherwise bind the sample compound, has been proposed as an additional reason for improved sample peak shape [13].

The purpose of the present reported work is to investigate the process by which solvents such as THF reduce the bandwidth and tailing of eluted sample peaks. The sorbent Hamilton PRP-∞ is employed because it is nominally nonporous and therefore is composed of only polymer matrix, free of macropores [16]. Binary and ternary aqueous–organic solvent mixtures are used which contain MeOH and/or THF as the organic modifier. The following relationships are measured: equilibrium sorption isotherms and sorption rate curves for the sample compound naphthalene (NA); equilibrium sorption isotherms of the solvent components MeOH and THF from aqueous solution; and equilibrium swelling of PRP-∞ as a function of the concentrations of MeOH and THF in aqueous solution.

2. Theory

2.1. Activity of organic modifier in solution

When a binary aqueous–organic solvent mixture is employed as a mobile phase, the organic modifier is selectively sorbed by the polymer. A plot of concentration sorbed against concentration in solution at a fixed temperature is the sorption isotherm of the modifier. Sorption occurs because of free energy and spatial changes which occur upon transfer of an organic modifier molecule from one phase into the other [24]. If it is desired to know how the contribution to sorption by the polymer phase alone differs at different points along the isotherm, it is necessary to plot activity of the modifier in the solution phase, rather than its concentration [25].

Activity coefficients (pure-solute standard state) for MeOH in MeOH–H_2O were calculated using the Margules equation [26]:

$$\ln\gamma_1 = [A_{12} + 2(A_{21} - A_{12})\chi_1]\chi_2^2 \quad (1)$$

where γ_1 is the activity coefficient of the organic modifier; χ_1 is its mole fraction; χ_2 is the mole fraction of water; and A_{12} and A_{21} are constants from the literature [27]. Activity coefficients for THF in THF–H_2O were calculated using the nonrandom, two liquid (NRTL) equation [28]:

$$\ln\gamma_1 = \chi_2^2[\tau_{21}\, G_{21}^2\, (\chi_1 + \chi_2\, G_{21})^{-2} + \tau_{12}\, G_{12}^2\, (\chi_2 + \chi_1\, G_{12})^{-2}] \quad (2)$$

where the parameters τ_{12}, τ_{21}, G_{12}, and G_{21} are constants obtained from the literature [29]. Plots of γ_1 versus weight-volume concentration in aqueous solution, C_1, are shown in Fig. 1 for both MeOH and THF. Activities, a_1, are obtained as the product:

$$a_1 = \gamma_1\, \chi_1 \quad (3)$$

and χ_1 is calculated from C_1 by the relationship:

$$\chi_1 = \left[1 - \frac{m_1}{m_2}\left(1 - \frac{\rho_{mix}}{C_1}\right)\right]^{-1} \quad (4)$$

where m_1 and m_2 are molar masses and ρ_{mix} is the

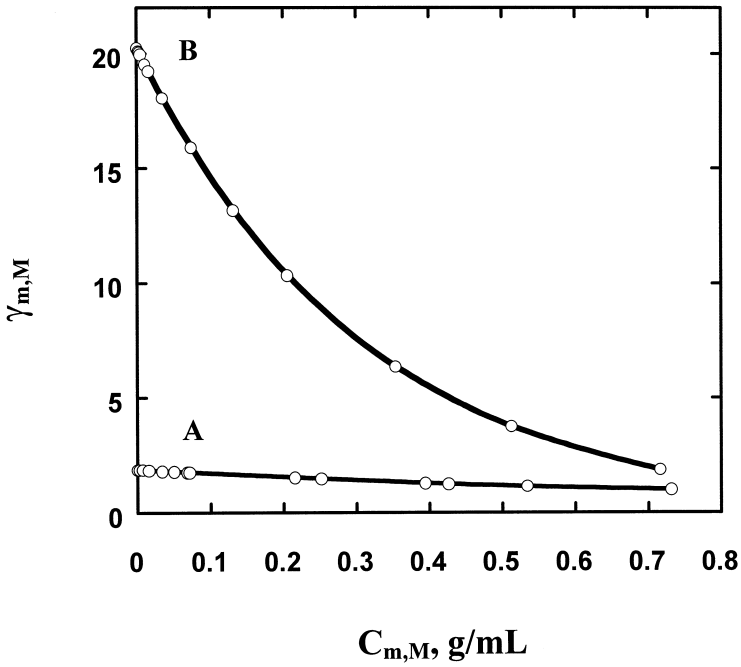

Fig. 1. Change in activity coefficients with change in weight-volume concentrations in aqueous solution for MeOH (A) and THF (B).

density of the solution whose value as a function of C_1 can be found from the literature [30].

2.2. Polymer structure

Polymers such as PRP-∞ which are synthesized by suspension polymerization of a mixture of vinylbenzene (styrene) and divinylbenzene monomers in the absence of both solvent- and porogen-diluents are considered to be composed of a solid, nominally nonporous, matrix which is heterogeneous with respect to crosslinking density, chain density and swelling properties. The following structure is envisaged [11,31–34]: throughout the polymer particle is a very large number of very small and closely spaced nuclei (or ''nodules''). The crosslinking density and chain entanglements are highest within the nuclei and decrease with distance from the nuclei. Thus, there is a gradient of crosslinking density from the center of each nucleus to the internuclear region. Regions of the matrix having higher crosslinking density have greater rigidity and contain larger and more numerous permanent spaces between the chains, (i.e. permanent micropores). Micropores are defined as having diameters $\leq$2 nm [11]. Regions with lower crosslinking density are more flexible and are called gel.

In the dry state, with no sorbed organic solvent, the gel regions of the matrix collapse completely into a structure having the smallest possible spaces between the chains; but the micropore regions are unable to collapse, so that they retain their permanent microporosity. However, in the solvent-swollen condition, the gel regions are extensively swollen and have larger interchain pore spaces than do the micropore regions that do not swell much.

2.3. Sample diffusion in polymer matrix

Since the particles of PRP-∞ were preequilibrated with the solvent mixture and since the concentration of the sample compound was within the linear region of its sorption isotherm, solvent uptake and polymer swelling were already at equilibrium, and no measurable additional swelling accompanied the sorption of sample. If the spherical PRP-∞ particle behaves as a homogeneous medium, then the rate of sample

sorption can be described by the expression [16,35,36]:

$$F = \frac{n_t}{n_\infty} = 1 - \frac{6}{\pi^2}\sum_{m=1}^{\infty}\frac{1}{m^2}\exp\left(-m^2\,\pi\,\frac{D}{r^2}\,t\right) \qquad (5)$$

in which F is the fraction of the equilibrium amount of sample sorbed at time, t; n_t and n_∞ are the moles of sample sorbed per dry gram of PRP-∞ at time t and at equilibrium, respectively; m is an integer; r is the radius of the particle; and D is the diffusion coefficient of the sample within the particle. Although PRP-∞ is actually heterogeneous with regard to crosslinking density, solvent sorption, swelling and permanent microporosity, the distances between the centers of the polymer nuclei are so small that an average value of D is adequate to describe diffusion.

If, in a polymer matrix, the polymer volume fraction, ϑ, is high, diffusion is limited by the free-volume (i.e. $1-\vartheta$) [37–39]. The diffusion coefficient of a solute in the polymer matrix in the presence of solvent (D), can be related to that in the dry polymer matrix (D_p) by the equation:

$$D = \frac{D_p\lambda}{\theta} \qquad (6)$$

where λ is the ratio of the hindrance parameters and Θ is the ratio of tortuosities, in the presence and absence of solvent. Hindrance depends on the ratio of solute radius to pore radius. Under swelling conditions this ratio decreases, meaning hindrance has decreased. In Eq. (6), a decrease in hindrance is reflected as an increase in λ. Swelling also reduces tortuosity, causing Θ to get smaller, though only marginally so.

If, for simplicity, the continuum of crosslinking densities in the matrix is approximated by only two degrees of crosslinking, one representing all gel and one representing all permanent micropores, then the relative contributions to the hindrance and tortuosity can be defined by:

$$\lambda^{-1} \simeq \frac{n_{gel}\lambda_{gel}^{-1} + n_\mu\lambda_\mu^{-1}}{n_{gel} + n_\mu} \qquad (7)$$

and

$$\theta \simeq \frac{n_{gel}\theta_{gel} + n_\mu\theta_\mu}{n_{gel} + n_\mu} \qquad (8)$$

where n_{gel} and n_μ are the sorption capacities of the gel and micropore regions, respectively. Eqs. (7) and (8) are employed later to estimate, separately, the effects of swelling solvents on λ and Θ.

2.4. Predicted elution peaks

A mathematical method was developed previously, by which an experimentally measured sample sorption rate curve may be used to accurately predict the contribution of intraparticle diffusion to the shape of the peak that would be obtained when the sample elutes from a liquid chromatographic column [5,15]. In this approach, the sorption rate curve, such as might be described by the theoretical Eq. (5), is fit by an *empirical* biexponential equation of the form:

$$F = 1 - \frac{n_1}{n_0}\exp(-k_1\,t) - \frac{n_2}{n_0}\exp(-k_2\,t) \qquad (9)$$

in which n_1 and n_2 are the moles of sample sorbed at equilibrium whose sorption rates can be described by the first-order rate constants k_1 and k_2, respectively. Here, n_1 and n_2 are not necessarily synonymous with n_{gel} and n_μ. The chromatographic column is then imagined to be composed of two ''hypothetical columns'' in series, on which n_1 and n_2 are proportional to the number of sorption sites and $n_0 = n_1 + n_2$. The hypothetical peak eluting from each hypothetical column is calculated from equations of Giddings [40]. Numerical convolution of the two hypothetical peaks leads to the overall predicted elution peak shape contribution from intraparticle diffusion.

This approach makes it easy to predict how changes in the shape of the measured sorption rate curve will be reflected in changes in bandwidth and tailing of the chromatographic peak for an eluted compound.

3. Experimental

3.1. Reagents, solvents, and resin

NA, phloroglucinol, NANO–pure water, and MeOH were as previously described [5,15]. For swelling and solvent isotherm studies, THF (Caledon, Georgetown, ON, Canada) was reagent

grade and filtered through a 0.45 μm Nylon 66 membrane filter. For NA sorption isotherm and sorption rate studies, THF was distilled over Na(s), passed through a column of alumina, and filtered through a 0.45 μm Nylon 66 membrane before use. Blue dextran (Sigma) was used as received.

Binary aqueous–organic solvents of MeOH–H_2O and THF–H_2O, which were used to measure both sorption isotherms of the organic modifier and swelling of PRP-∞, were prepared by diluting known weights of the organic modifier to volume with water in a volumetric flask. Binary and ternary aqueous–organic solvents, such as 1:6:3 THF–MeOH–H_2O, which were used as solvents to measure sorption isotherms, sorption rates, and diffusion coefficients for the sample compound NA, were prepared by combining solvent volumes in the specified proportions.

The sorbent, PRP-∞ (Hamilton, Reno, NV, USA; batch EE2), is a nominally nonporous PS–DVB copolymer having a spherical particle diameter of 19±1 μm, as in Ref. [16].

3.2. Apparatus and procedure

3.2.1. Solvent sorption isotherms

A mass, W_p(=0.0793 g), of dry PRP-∞ was loosely packed into a 0.20 cm I.D.×5.0 cm long glass column with polypropylene end fittings and 2 μm pore-size stainless steel frits (Chromatronix, Type MB). The column was thermostatted at 25.0±0.5°C in a water bath (Lauda K4R, Brinkman). Three constant pressure pumps [41] were connected to the column inlet by PTFE tubing, through a six-port rotary valve (Cheminert). The three pumps contained, respectively: MeOH, for initially wetting the dry PRP-∞; the aqueous–organic solvent of interest for equilibration with the PRP-∞; and water, for eluting the sorbed organic modifier from PRP-∞. The outlet of the glass column was connected to a three-port slider valve (Cheminert) which permitted the effluent from the column to be directed either to waste, during the wetting and equilibration steps, or to a volumetric flask of volume, V_E, during the elution step. The eluate was collected to volume. Complete elution of sorbed organic modifier was verified by collecting fractions. The eluate in the volumetric flask was mixed and then it was pumped by a peristaltic pump (Gilson, Minipuls 2) through a differential refractometric chromatographic detector (Series R-400, Waters) in order to measure the concentration, $C_{m,E}$ (g/ml), of organic modifier in the eluate. Conversion of $C_{m,E}$ into the concentration of organic modifier that had been sorbed per gram of PRP-∞, $C_{m,S}$ (g/g), was done as described in Ref. [5], with blue dextran being used as the unretained component to correct for hold-up volume.

To facilitate later comparison with polymer swelling, $C_{m,S}$ was converted to the volume sorbed, $V_{m,S}$, by the equation:

$$V_{m,S} = \frac{C_{m,S}\,\bar{V}_m\,N_{av}}{\bar{M}_m} \tag{10}$$

in which $\bar{M}_m$ is the gram molecular weight of the organic modifier, N_{av} is Avogadro's number, and $\bar{V}_m$ is the volume of one molecule of organic modifier, as obtained from the software program Molecular Modeling (Windowchem Software).

3.2.2. Swelling of polymer

Swelling of individual particles of PRP-∞ was measured microscopically at room temperature in a flat flow-through cell. The solvent of interest was pumped slowly through the cell for 1 h to guarantee that the particles had come to equilibrium with the solvent. The cell was then disconnected from the pump, the inlet and outlet tubes were plugged with PTFE stoppers, and it was placed on the stage of a Leizt/Wetzlar Ortholux-Pol microscope fitted with a 125× reflective, long working distance (4 mm) objective (Leizt ∞/0, plan, L125X/0.80 N.A.) and a 10× eyepiece which contained a scale (Bausch and Lomb Optical). The smallest scale division corresponded to 0.7 μm so that length could be estimated to ±0.1 μm. Transmitted light from an incandescent source was passed through a substage condenser. The diameter of each particle in the horizontal plane was measured in four orientations, which were averaged in order to compensate for any slight deviations from perfect sphericity. The relative standard deviation of measurement in a given orientation was found to be 0.5% by a multiple focus–defocus technique [42]. Because the particles tended to adhere to the inner surface of the glass cell without being dislodged by the gently flowing solvent, it was

easy to keep track of the individual particles through many changes of solvent and microscopic measurements.

Solvent compositions were changed successively from low to high concentration for each organic modifier, MeOH and THF, in water. The diameter of the particle, d_m, observed in a given aqueous–organic solvent was converted to a fractional volume swelling, Q, by the equation:

$$Q = \left[\left(\frac{d_m}{d_w} \right)^3 - 1 \right] \quad (11)$$

where d_w is the diameter in pure water. The volume increment per unit dry mass of particles, ΔV_p, is given by:

$$\Delta V_p = \frac{Q \frac{4}{3} \pi \left(\frac{d_w}{2} \right)^3}{\rho_{PRP-\infty}} \quad (12)$$

in which $\rho_{PRP-\infty}$ is the density of dry PRP-∞ (=1.05 g/cm^3), as measured from the volume of aqueous blue dextran solution displaced by a known weight of PRP-∞.

3.2.3. Sample sorption isotherms and sorption rate curves

Both the sorption equilibrium and sorption rate studies for NA were performed using the shallow-bed apparatus which was previously described [15], with the detector being a Lambda-Max model 481 UV-absorbance detector (Waters) set at 276 nm. The weight of PRP-∞ in the shallow bed was about 3 mg, accurately weighed. Eight different shallow beds were employed over the course of the isotherm and kinetic studies. Temperature was thermostatted at 25.0±0.5°C.

Sample sorption isotherms were measured by the ''column equilibration technique'' [43]. A solution of NA at concentration $V_{i,M}$ (ml$_i$/ml$_M$) in the aqueous–organic mobile phase of interest was pumped through the 3 mg bed of PRP-∞ for 90 min, a time sufficient to guarantee that sorption equilibrium was achieved. $V_{i,M}$ was calculated by an equation analogous to Eq. (10), with $\bar{V}_i = 1.31 \cdot 10^{-22}$ ml/molecule. The bed of PRP-∞ was then switched out of the sample solution stream and into the eluent stream, which had the same composition as the mobile phase. The eluate from the bed of PRP-∞ flowed through the HPLC column to the UV detector. The amount of NA eluted was corrected for the hold-up volume of the shallow bed as described in [5], using phloroglucinol as the unretained component. This gave the volume of NA sorbed per gram of PRP-∞, $V_{i,S}$ (ml/g). The hold-up volume was typically about 0.01 ml. The sorption isotherm of the sample component, i, was obtained by repeating the column equilibration measurement at several concentrations of i in a mobile phase of fixed aqueous–organic solvent composition.

Sample sorption rate curves were measured by the shallow-bed technique on the same 3 mg beds of PRP-∞. The procedure was the same as just described for sorption isotherm measurements except that the length of time that the sample solution was allowed to flow through the bed of PRP-∞ was varied between 10 s and 3600 s. Other details of the kinetic technique, such as experimentally verifying the attainment of shallow-bed conditions, have been described previously [15] and were employed in this study.

3.2.4. Measurement of diffusion coefficients

Bulk solution diffusion coefficients of NA were measured in aqueous–organic solvents at 25.0±0.2°C by the Taylor dispersion method, using an apparatus which has been previously described [44].

4. Results and discussion

4.1. Solvent sorption isotherms

Shown in Fig. 2 are sorption isotherms for both organic modifiers, MeOH and THF, plotted as volume of organic modifier sorbed per gram of PRP-∞ ($V_{m,S}$, ml/g) versus activity in solution ($a_{m,M}$). The values employed for $\bar{V}_m$ in the calculation of $V_{m,S}$ via Eq. (10) were $3.62 \cdot 10^{-23}$ ml/molecule for MeOH and $7.46 \cdot 10^{-23}$ ml/molecule for THF.

Conventionally, sorption isotherms are plotted versus solution concentration [18,45,46]. However, since high solution concentrations of organic modifier sorbate are involved in the present work, solution phase activities ($a_{m,M}$) must be used in order for the

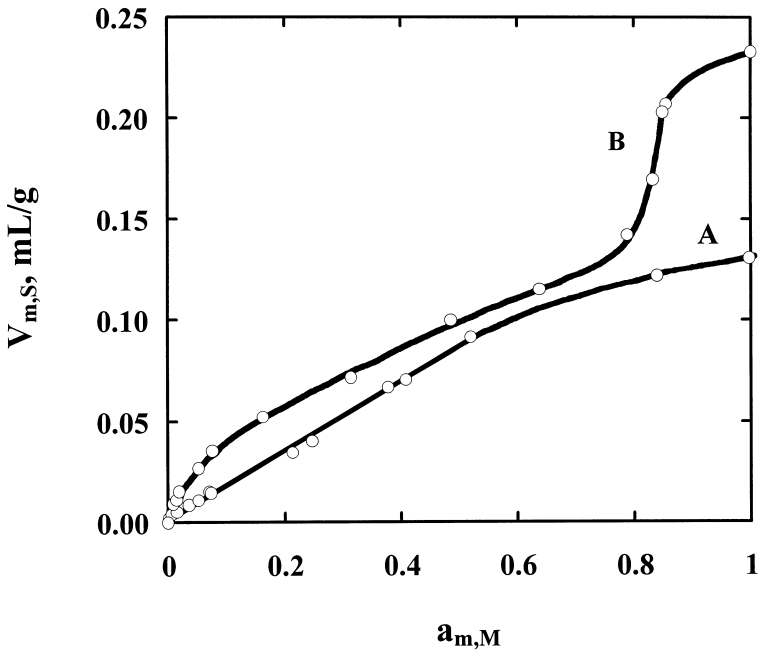

Fig. 2. Sorption isotherms for MeOH (A) and THF (B) on PRP-∞, using solution phase activities. Solid lines are empirical fits to the data.

isotherm to reflect only processes occurring in the sorbent phase.

If MeOH and THF were adsorbed only on the outside of the 19 μm diameter particles, then on 1.00 g (i.e. $2.6 \cdot 10^8$ particles) of PRP-∞, a close-packed monolayer of these sorbates would contain only $5.6 \cdot 10^{-5}$ ml/g for MeOH or $6.4 \cdot 10^{-5}$ ml/g for THF. Since all of the experimental points in Fig. 2 have values of $V_{m,S}$ that are far above these values, it is clear that most of the sorbed MeOH and THF are in the polymer particle rather than on the particle surface.

For MeOH sorption, the isotherm in Fig. 2A is nearly linear up to a point with coordinates $V_{MeOH,S} \approx 0.1$ ml/g and $a_{MeOH,M} \approx 0.6$, above which it becomes convex and levels off at a limiting value of $V_{MeOH,S} = 0.13$ ml/g at $a_{MeOH,M} = 1.00$ (i.e. in pure MeOH). For THF sorption, the isotherm in Fig. 2B is convex up to $a_{THF,M} \approx 0.8$ where $V_{THF,S} \approx 0.13$ ml/g. Above this point, the THF isotherm exhibits a strong upward concavity which persists to about $V_{THF,S} \approx 0.21$ ml/g, at which it again becomes convex and reaches its limiting value of $V_{THF,S} = 0.23_3$ ml/g at $a_{THF,M} = 1.00$ (i.e. in pure THF).

The overall shape of the THF sorption isotherm in Fig. 2B is similar in shape to the Brunauer Type IV [47] gas–solid isotherm that has been reported in the literature for adsorption of nitrogen gas on macroporous PS–DVB polymers [48]. In gas–solid adsorption from a single-component gas, the upward concavity followed by a levelling off is the result of multilayer adsorption in micropores and complete filling of these pores by ''capillary condensation'' [49,50]. In the present case of liquid–solid sorption, capillary condensation of THF is possible because only one of the two components of the binary solvent THF–H_2O enters the polymer matrix [49,51,52].

The fact that a concave upturn is completely absent from the MeOH isotherm (Fig. 2A) implies a lack of multilayer sorption and capillary condensation of MeOH in the permanent micropores of PRP-∞. The criteria for capillary condensation are embodied in the Kelvin equation [50,53,54], an examination of which shows that the difference in behavior of MeOH and THF lies in the higher surface tension and molar volume of THF. For a particular size pore, the equilibrium vapour pressure, which is proportional to activity in solution, that is required for the onset of capillary condensation is lower for THF than for MeOH.

4.2. Polymer swelling

A variety of experimental techniques have been described in the literature to measure the dependence of swelling of polymeric sorbent particles on mobile phase solvent composition [20,31,55–59]. Only microscopy gives a direct measurement of particle swelling and is the technique employed in the present study.

Shown in Fig. 3 are swelling curves for both MeOH and THF, plotted as volume increase per gram of PRP-∞ (ΔV_p, ml/g) versus activity of the organic modifier in the solvent ($a_{m,M}$). Both of the swelling curves are convex, with the THF curve falling about twice as high as the MeOH curve except at $a_{m,M} \leq 0.05$ where the two curves are superimposed. At $a_{THF,M} \approx 0.8$, swelling is seen to increase sharply and then level off as THF experiences capillary condensation. Since the capillary condensation seen in this region of the curve is accompanied by some swelling, the condensation is occurring in permanent micropores that are not the most highly crosslinked ones. The amount of swelling experienced by a PS–DVB polymer at equilibrium represents a balance between the interaction energy for solvation of the polymer chains by the organic solvent and elastic forces of the polymer network. The solvation energy is greater for a smaller difference between the solubility parameters of the polymer and the organic modifier [31,32,57] and for a higher activity of the organic modifier in the aqueous solution, while the elastic force is greater for a higher crosslinking density in the polymer [31,32,57,60–62]. A more detailed understanding of the changes occurring in the polymer with solvent sorption requires a comparison of the swelling curves with the sorption isotherms.

4.3. Swelling versus solvent sorption

Shown in Figs. 4 and 5 are plots of ΔV_p versus $V_{m,S}$ for MeOH–H_2O and THF–H_2O, respectively. The points on these plots are from the corresponding vertical axis in Figs. 2 and 3. Thus, $a_{m,M}$ cancels out and the plots in Figs. 4 and 5 show the volume swelling produced by the volume sorbed. All swell-

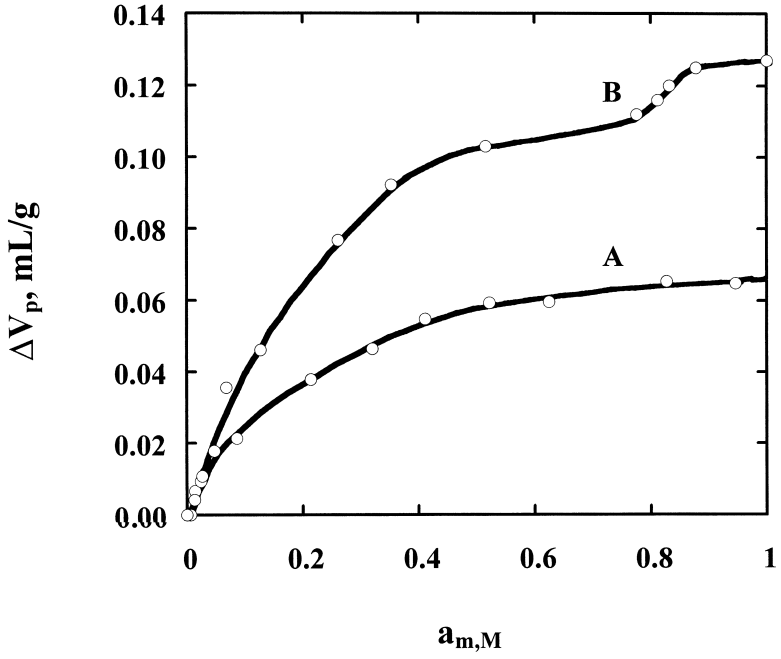

Fig. 3. Swelling of PRP-∞ produced by the sorption of MeOH (A) and THF (B) at different solution phase activities. Solid lines are empirical fits to the data.

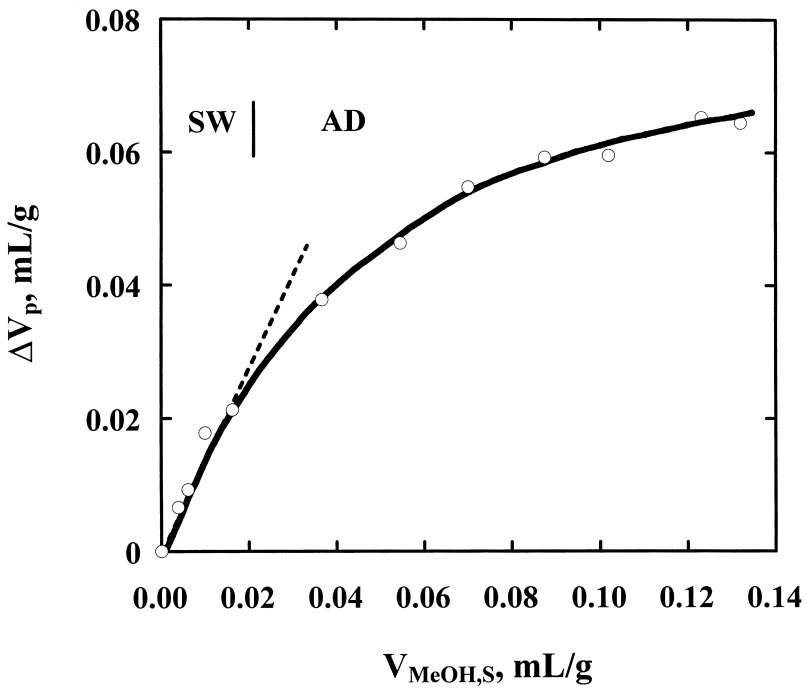

Fig. 4. Swelling produced by sorbed volume of MeOH on PRP-∞. Solid line is empirical fit to the data. The dashed straight line identifies the linear, external swelling region.

ing is due to MeOH or THF since water is not sorbed by the polymer matrix [63].

When the sorbed organic modifier causes only ''external'' or ''isotropic'' [18,64] swelling, in which the polymer gel expands without loss of any of the permanent porosity that was present in the dry matrix, the points will fall on a straight line. This is seen in region SW of Fig. 4, the swelling versus sorption curve for MeOH. At sorbed volumes above $V_{\mathrm{MeOH,S}} \approx 0.02$ ml/g, region AD in Fig. 4, the negative deviation from linearity indicates that the predominant process is sorption of MeOH into permanent micropores [18].

At low sorbed volumes of THF, up to ~0.01 ml/g, little or no measurable swelling of the polymer occurs with sorption. This is indicated by region AD_1 in Fig. 5. In this region, THF is experiencing multilayer sorption and capillary condensation. The fact that this occurs at a very low $a_{\mathrm{THF,M}}$ and is not accompanied by swelling implies that this condensation is occurring in the smallest, most highly cross-linked of the permanent micropores. In the next region in Fig. 5, which is labelled SW and is fit with a dashed straight line, sorbed THF causes external swelling of the gel. Above a sorbed volume of 0.08 ml/g, region AD_2 in Fig. 5, the predominant process is again THF entering the micropores. From the THF isotherm in Fig. 2B, it is seen that multilayer sorption and capillary condensation occur within the micropores at sorbed volumes above 0.13 ml/g. CC indicates this region in Fig. 5.

4.4. Sample sorption isotherms

Shown in Fig. 6A is the isotherm for the sorption of the sample compound NA on PRP-∞ from 0:7:3 THF–MeOH–H_2O. The vertical axis units are ml NA per gram of PRP-∞ and the horizontal axis units are ml NA per ml of solution. The solid line represents the nonlinear least squares fit to the data by the ''solubility-limited Langmuir'' equation [46]:

$$V_{i,\mathrm{S}} = \frac{V_{i,\mathrm{S,max}}\, K_{\mathrm{ads}}\, \frac{V_{i,\mathrm{M}}}{V_{i,\mathrm{sat}}}}{1 + (K_{\mathrm{ads}} - 1)\, \frac{V_{i,\mathrm{M}}}{V_{i,\mathrm{sat}}}} \tag{13}$$

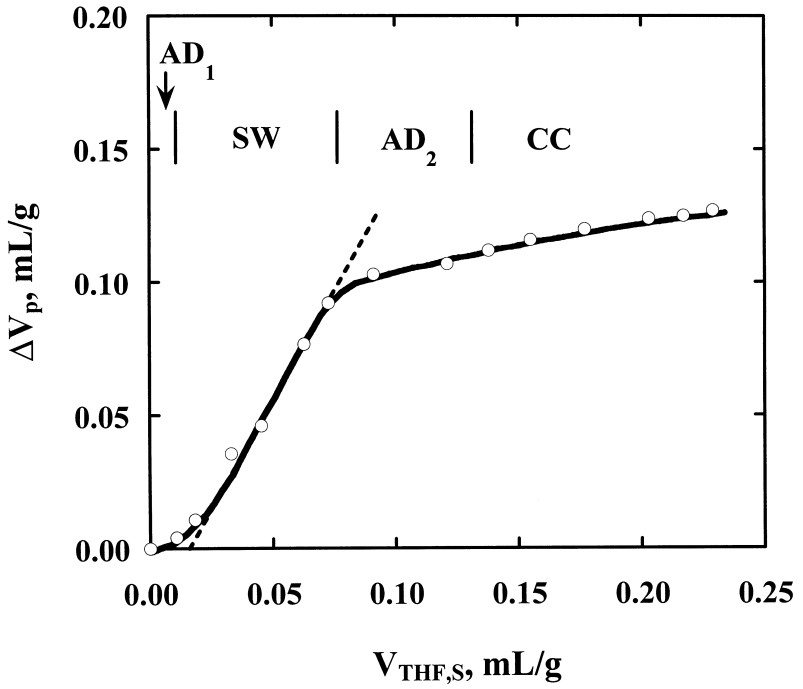

Fig. 5. Swelling produced by sorbed volume of THF on PRP-∞. Solid line is empirical fit to the data. The dashed straight line identifies the linear, external swelling region.

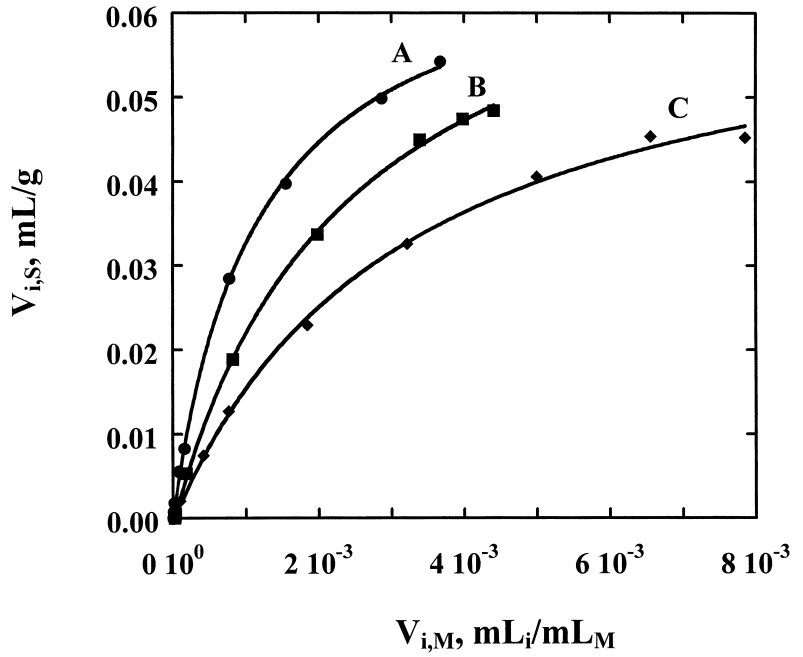

Fig. 6. Sample sorption isotherms of naphthalene on PRP-∞ from different composition solvents: 0:7:3 THF–MeOH–H_2O (A); 0.2:6.8:3 THF–MeOH–H_2O (B); 1:6:3 THF–MeOH–H_2O (C). The data have been fit by the solubility-limited Langmuir isotherm equation.

where K_{ads} is the thermodynamic equilibrium constant and $V_{i,sat}$ is the volume concentration of sorbate in the saturated solution. Since the solution concentrations of NA are small, its activity coefficient is approximately constant and concentrations are proportional to activity. The highest point on the isotherm, $V_{i,S,max}$, is the sorption capacity of PRP-∞ and is proportional to the total number of sorption sites. For a solubility-limited isotherm, $V_{i,S,max}$ is measured using a saturated solution of NA, in which $a_{i,M}=1.00$. Since PRP-∞ is at equilibrium with a saturated solution of NA, it is necessarily at equilibrium with pure NA. Curve B in Fig. 6 is the NA isotherm obtained using 0.2:6.8:3 THF–MeOH–H_2O solvent, and Curve C is the NA isotherm obtained using 1:6:3 THF–MeOH–H_2O solvent, both of which have been fit to the solubility-limited Langmuir equation.

The fitting parameters for the three NA isotherms are presented in Table 1. Differences in the values of $V_{i,S,max}$ that are observed among the three solvents can arise only from a difference in the number of sorption sites in PRP-∞. This number decreases by 11% and by 17% upon going from 0% THF to 2% THF and 10% THF, respectively. The parameter $\frac{K_{ads}}{V_{i,sat}}$ on the other hand, is related only to differences in overall free-energy of transfer from solution phase into polymer phase. A difference in this parameter for NA in different solvents can arise from differences in solvent strength of the solution phase and/or from differences in sorption energy per sorption site in the polymer phase. The 60% decrease in $\frac{K_{ads}}{V_{i,sat}}$ in the 1:6:3 solvent compared to the 0:7:3 solvent is larger than the 12% decrease expected from the increase in solvent strength that is predicted from the Polarity Index (P')-based semiempirical model of Snyder, using volume weighting of P' for the binary and ternary mixed solvents [65,66]. This greater-than-predicted effect suggests that the presence of THF not only increases the solvent strength in the solution phase but may also decrease the sorption energy per sorption site in the polymer phase.

4.5. Sample sorption rate

Shown as data points in Fig. 7 are the sample sorption rate curves for NA on PRP-∞ from 0%, 2% and 10% THF in MeOH–H_2O. The sorption rate curves were measured within the linear regions of the respective isotherms, at a concentration of NA of $9.7\cdot10^{-5}$ *M*. The curves have been plotted as the fractional attainment of the equilibrium amount sorbed versus time. The solid lines are the nonlinear least squares fits of n_t versus t by Eq. (5), representing diffusion through a homogeneous sphere. The fitting parameters, n_∞ and D, are given in columns 3 and 4 in Table 2. The diffusion coefficient of NA through the polymer increased by 90% upon changing from 0% THF to 2% THF, and by additional 20% upon increasing to 10% THF. As seen in the footnote of Table 2, the increase in the diffusion coefficient of NA within the polymer, upon the addition of THF to the mobile phase, is not accompanied by a corresponding change in the free-solution diffusion coefficient.

4.6. Elution peaks

In order to use the previously developed model for the prediction of elution peaks [5,15], the sorption rate data in Fig. 7(A–C) were fit to Eq. (9), an empirical biexponential equation. The biexponential fits, which for clarity are not shown in Fig. 7, were comparable in quality to the fits of Eq. (5) to the data. The parameters from the biexponential fits are given in Table 3. The k' values necessary for the predictions were calculated from the slope of the linear region of the isotherms, κ, via the equation:

Table 1
Curve fitting parameters from fit of Eq. (13) to sample sorption isotherm data in Fig. 6

Curve	Solvent (THF–MeOH–H_2O)	$V_{i,sat}$ (ml_i/ml_M)	$V_{i,S,max}$ (ml/g)	$\frac{K_{ads}}{V_{i,sat}}\cdot10^2$
A	0:7:3	0.00367	0.0542±0.0003	11.4
B	0.2:6.8:3	0.00439	0.0484±0.0006	6.4
C	1:6:3	0.00784	0.045±0.001	4.3

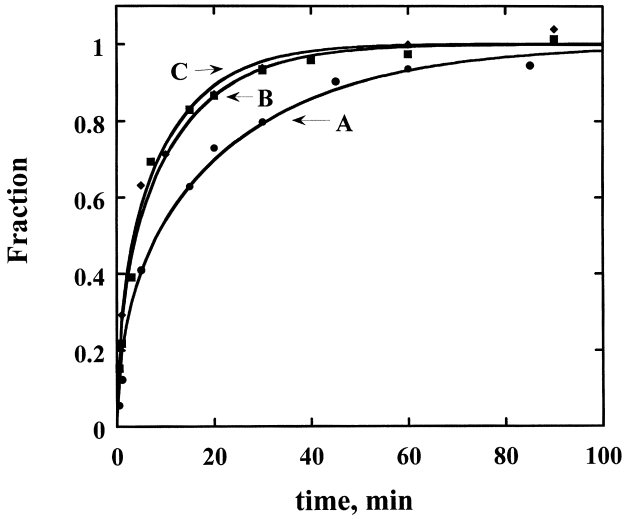

Fig. 7. Sample sorption rate curves of naphthalene on PRP-∞ from different composition solvents: 0:7:3 THF–MeOH–H_2O (A); 0.2:6.8:3 THF–MeOH–H_2O (B); 1:6:3 THF–MeOH–H_2O (C). The data have been fit by Eq. (5). Concentration of NA in solution was $9.7\cdot10^{-5}$ *M*, within the linear region of the isotherms.

Table 2
Curve fitting parameters from fit of Eq. (5) to sample sorption rate data in Fig. 7

Compound	Solvent (THF–MeOH–H_2O)	n_∞ (mol/g)·10^6	D (cm^2/s)·10^{11}
NA	0:7:3	9.2±0.4	7±1
NA	0.2:6.8:3	6.5±0.2	13±2
NA	1:6:3	2.92±0.05	15±1

Bulk solution diffusion coefficients of NA in 0:7:3 THF–MeOH–H_2O and 1:6:3 THF–MeOH–H_2O are $(6.4\pm0.1)\cdot10^{-6}$ cm^2/s and $(6.6\pm0.1)\cdot10^{-6}$ cm^2/s, respectively, as measured by the Taylor dispersion method.

$$k' = \kappa\frac{W_{col}}{V_M} \tag{14}$$

where $W_{col}=1.36$ g is the mass of PRP-∞ in a 4.1×150 mm column and $V_M=0.73$ ml is the void volume [67]. The k' values for NA were calculated to be 197.1, 93.9 and 46.3 for mobile phases containing 0%, 2% and 10% THF in MeOH–H_2O, respectively.

Shown in Fig. 8 are the predicted elution profiles for NA eluting from the column of PRP-∞ at a mobile phase linear velocity of 0.0013 cm/s. The predicted peaks have been plotted as the normalized signal, where the area under the curve is equal to one, versus the normalized retention time, where t_r is taken as the center of gravity of the peak. The excessive band broadening and tailing is quite pronounced when no THF is present. The predicted profile becomes narrower when 2% THF is included in the solvent due to the increase in the intraparticle diffusion coefficient. Changing to 10% THF produces little further change in peak shape, con-

Table 3
Curve fitting parameters from fit of Eq. (9) (empirical biexponential equation) to sample sorption rate data in Fig. 7 (not indicative of significant digits)

Compound	Solvent (THF–MeOH–H_2O)	$n_0\cdot10^6$	$n_1\cdot10^6$	k_1	$n_2\cdot10^6$	k_2
NA	0:7:3	9.101	1.122	2.618	7.98	0.08721
NA	0.2:6.8:3	6.542	4.013	0.3207	2.53	0.05471
NA	1:6:3	3.007	1.46	0.8523	1.547	0.05672

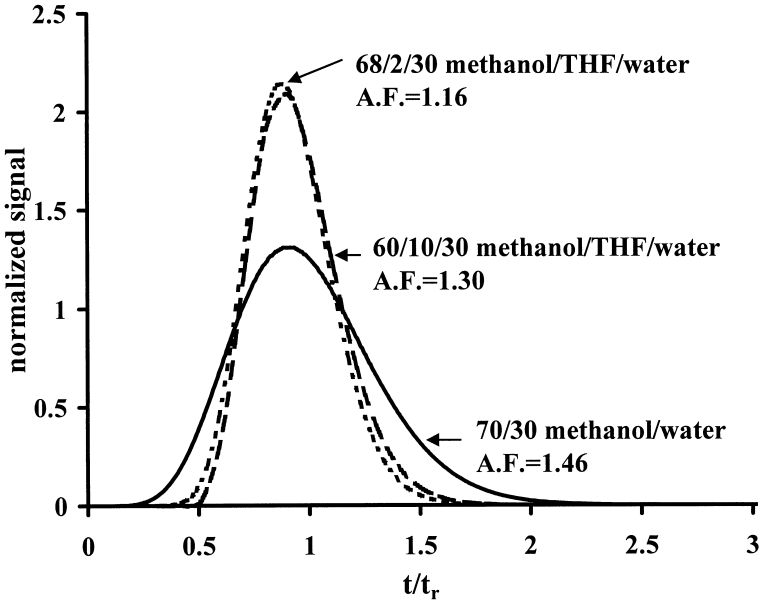

Fig. 8. Predicted elution profiles for NA at a linear velocity of 0.0013 cm/s from a 4.1×150 mm column of PRP-∞, using parameters obtained from empirical biexponential fits to sorption rate data.

sistent with only a small further increase in *D*. The predicted improvement in peak shape seen in Fig. 8 is qualitatively similar to that which was experimentally observed [12]. Quantitatively, the peaks in Fig. 8 are different from those in Ref. [12] because the PRP-∞ particles that are assumed in the prediction are larger and are not macroporous.

4.7. Effect of THF on the polymer matrix

It is shown above that sorption of THF by PRP-∞ is accompanied by three changes: (i) increased swelling, (ii) decreased sorption capacity for the solute NA, and (iii) increased diffusion coefficient of the solute in the polymer. It is also shown that the third of these changes is responsible for the improvement in chromatographic peak shape of the solute. The first two changes are in some way the cause of the third. Conceptually, the possible influence of swelling and sorption capacity on solute diffusion coefficient can be expressed in terms of Eqs. (6)–(8). Increased swelling will have little effect on Θ (Eq. (8)), because tortuosity typically has a narrow range of values [68,69]. Greater swelling could increase λ_{gel} but would have little effect on λ_{μ}; while smaller capacity would mean a smaller value of n_{gel}, n_{μ} or both.

The chromatography literature [12,13,19–21] suggests that the improvement in peak shape which is observed in the presence of THF is due to increased polymer swelling. To test this hypothesis, PRP-∞ particle size was measured in 0%, 2% and 10% THF in MeOH–H_2O. The resulting increases in particle volume over the dry particle volume were 6.4±0.1%, 6.77±0.01%, and 11.1±0.8%, respectively, while the diffusion coefficients of NA in these solvent-equilibrated particles were $7\cdot10^{-11}$, $13\cdot10^{-11}$ and $15\cdot10^{-11}$ cm^2/s, from Table 2. Thus, an increase in particle volume of 0.4%, upon adding 2% THF, corresponds to the 90% increase in the value of *D*, while a further increase of over 4% in volume upon changing to 10% THF corresponds to the additional 20% increase in *D*. Hence, the increase in *D*, which is observed upon adding THF, does not correlate with the swelling. This implies that 0:7:3 THF–MeOH–H_2O solvent has already caused the gel regions of the polymer matrix to swell sufficiently that hindrance to diffusion in the gel is small and $(n_{gel}\lambda_{gel}^{-1}) \ll (n_{\mu}\lambda_{\mu}^{-1})$. This view is supported

by the fact that 0:7:3 THF–MeOH–H_2O, in which the activity of MeOH is 0.61, falls on the plateau in the MeOH swelling curve (A) in Fig. 3.

This leaves the term ($n_\mu \lambda_\mu^{-1}$) in Eq. (7) to explain the increase in D for NA in the presence of THF. Because permanent micropores do not swell, λ_μ does not change upon solvent sorption, so the decrease in n_μ, the sorption capacity in the micropores, is identified as being primarily responsible for the increase in D and the improved chromatographic peak shape which occurs upon sorption of THF by PS–DVB polymers. The 11% decrease in sorption capacity ($V_{i,S,max}$) that is produced upon changing from 0% THF to 2% THF and the further 6% decrease in capacity produced by changing to 10% THF correlate with the 90% and 20% increase in D that are observed.

The physico–chemical origin of this ''special'' behaviour of THF must be due to processes occurring in region AD_1 of Fig. 5, where the concentration of sorbed THF is small and it is being sorbed with almost no concomitant swelling of the polymer. Here, THF is experiencing self-association and capillary condensation in the smallest of the permanent micropores. These are significantly smaller than the majority of the micropores in which capillary condensation occurs at $a_{THF,M} \geq 0.8$ (Fig. 2), and therefore, these are the micropores in which, in the absence of THF, solute diffusion is most highly hindered, causing poor peak efficiency and tailing. The filling of these micropores by THF effectively blocks them to the entrance of solute molecules (NA). The volume associated with the blockage of these small, permanent micropores is about 0.01 ml/g (horizontal axis, Fig. 5), which corresponds to 10% of the 0.10 ml/g of MeOH sorbed from 0:7:3 THF–MeOH–H_2O (vertical axis, Fig. 2, at $a_{m,M} \approx$ 0.6). This correlates well with the 11% reduction in sorption capacity for NA on going from 0% THF to 2% THF in MeOH–H_2O (column 4, Table 1). Blockage of the kinetically most hindered micropores by THF is similar to that reported on silica gel where water is said to block the adsorption of molecules on slow sites [70], and is a mass-transfer analogue to the well-known blocking of thermodynamically active sites by water, also on silica gel [71].

5. Conclusion

Swelling of the gel region and of the larger micropores occurs upon sorption of all organic modifier solvents by PRP-∞. However, swelling does not occur significantly in the smallest, most highly hindered micropores and is not responsible for reducing the hindered diffusion of sample molecules in them. This reduction is due, rather, to ''blocking'' of these micropores by certain types of solvents, including THF. This blocking prevents the diffusion of sample molecules into the micropores. The fact that the slightly soluble sample compound NA exhibits a ''solubility-limited Langmuir'' isotherm, which is characterized by one equilibrium constant, suggests that the sorption energy of NA is the same in all three regions of the polymer (i.e. smallest micropores, larger micropores, and gel) which, in turn, implies that the sorption sites in all three regions are equally energetic. Therefore, the ''blocking'' of the micropores by solvents like THF is due not to ''selective binding'' of THF by the micropores [13], but rather to the properties of THF which cause it to self-associate and capillary-condense. The extra sorption energy of THF in the micropores comes from these processes.

It is very reasonable to assume that, qualitatively, the properties of PRP-∞ represent the properties of the polymer matrix in macroporous PS-DVB column packings such as PRP-1 and XAD-2. The macroporous packings are expected to be composed of gel, small micropores and larger micropores. However, it cannot be assumed, a priori, that the structure and properties of the polymer matrix in a macroporous packing will be quantitatively identical to those of PRP-∞. Thus, it is safe to expect that blocking of diffusionally hindered micropores by THF will be important in macroporous packings but it may be that the extra swelling caused by THF also contributes significantly to its ability to reduce sample peak width and tailing. Preliminary studies in this laboratory on two macroporous packings suggest that this may be true.

Acknowledgements

The Hamilton Co. kindly donated the sorbent

PRP-∞. This work was supported by the Natural Sciences and Engineering Research Council of Canada and the University of Alberta.

References

[1] R.L. Albright, React. Polym. 4 (1986) 155.
[2] L.L. Lloyd, J. Chromatogr. 544 (1991) 201.
[3] N. Tanaka, M. Araki, in: J.C. Giddings, E. Grushka, P.R. Brown (Eds.), Advances in Chromatography Selectivity and Retention in Chromatography, Vol. 30, Marcel Dekker, New York, 1989, p. 81.
[4] N. Tanaka, K. Kimata, K. Hosoya, H. Miyanishi, T. Araki, J. Chromatogr. A 656 (1993) 265.
[5] D. Gowanlock, R. Bailey, F.F. Cantwell, J. Chromatogr. A 726 (1996) 1.
[6] R.G. Baum, R. Saetre, F.F. Cantwell, Anal. Chem. 52 (1980) 15.
[7] H.J.E.M. Reeuwijk, U.R. Tjaden, J. Chromatogr. 353 (1986) 339.
[8] D.P. Lee, J. Chromatogr. Sci. 20 (1982) 203.
[9] D.P. Lee, J. Chromatogr. 443 (1988) 143.
[10] D. Liru, H. Xizhang, W. Qihui, M. Qingcheng, L. Yuliang, Z. Youliang, Sci. Sin. (Series B) 25 (1982) 905.
[11] F. Nevejans, M. Verzele, J. Chromatogr. 406 (1987) 325.
[12] L.D. Bowers, S. Pedigo, J. Chromatogr. 371 (1986) 243.
[13] N. Tanaka, T. Ebata, K. Hashizume, K. Hosoya, M. Araki, J. Chromatogr. 475 (1989) 195.
[14] J.V. Dawkins, L.L. Lloyd, F.P. Warner, J. Chromatogr. 352 (1986) 157.
[15] J. Li, L.M. Litwinson, F.F. Cantwell, J. Chromatogr. A 726 (1996) 25.
[16] J. Li, F.F. Cantwell, J. Chromatogr. A 726 (1996) 37.
[17] B.A. Brandrup, E.H. Immergut, Polymer Handbook, Wiley, New York, 1975.
[18] P. Cornel, H. Sontheimer, Chem. Eng. Sci. 41 (1986) 1791.
[19] R.M. Smith, D.R. Garside, J. Chromatogr. 407 (1987) 19.
[20] S. Coppi, A. Betti, C. Bighi, G.P. Cartoni, F. Coccioli, J. Chromatogr. 442 (1988) 97.
[21] H.W. Stuurman, J. Kohler, S.O. Jansson, A. Litzen, Chromatographia 23 (1987) 341.
[22] A.F.M. Barton, Handbook of Solubility Parameters and Other Cohesion Parameters, CRC Press, 1991.
[23] J.L. Gardon, in: H.F. Mark, N.G. Gaylord, N.M. Bikales (Eds.), Encyclopedia of Polymer Science and Technology, Interscience, New York, 1965, p. 833.
[24] J.G. Chen, S.G. Weber, L.L. Glavina, F.F. Cantwell, J. Chromatogr. A. 656 (1993) 549.
[25] W.E. Hammers, G.J. Meurs, C.L.d. Lignz, J. Chromatogr. 246 (1982) 169.
[26] M.S.B. Margules, Akad. Wiss. Wien, Math.—Naturwiss. KI. II 104 (1895) 1234.
[27] J. Gmehling, U. Onken, W. Arlt, Vapor-Liquid Equilibrium Data Collection, Aqueous-Organic System (Supplement 1), Chemistry Data Series, Vol. 1, part 1a, DECHEMA, Germany, 1981, p. 49.
[28] H. Renon, J.M. Prausnitz, AIChE J 14 (1968) 135.
[29] J. Gmehling, U. Onken, W. Arlt, Vapor-Liquid Equilibrium Data Collection, Aqueous-Organic System (Supplement 1), Chemistry Data Series, Vol. 1, part 1a, DECHEMA, Germany, 1981, p. 285.
[30] E.D. Katz, K. Ogan, R.P.W. Scott, J. Chromatogr. 352 (1986) 67.
[31] K.J. Shea, D.Y. Sasaki, G.J. Stoddard, Macromolecules 22 (1989) 1722.
[32] I.C. Poinescu, C. Beldie, C. Vlad, J. Appl. Polym. Sci. 29 (1984) 23.
[33] J.R. Millar, D.G. Smith, W.E. Marr, T.R.E. Kressman, J. Am. Chem. Soc. (1963) 218.
[34] K.J. Shea, G.J. Stoddard, Macromolecules 24 (1991) 1207.
[35] J. Crank, The Mathematics of Diffusion, Oxford University Press, 1975, Chapters 6 and 14.
[36] F. Helfferich, Ion Exchange, Mc-Graw Hill, New York, 1962, Chapter 6.
[37] A.H. Muhr, J.M.V. Blanshard, Polymer 23 (1982) 1012.
[38] J.S. Vrentas, J.L. Duda, J. Polym. Sci A2 15 (1977) 403.
[39] H. Fujita, in: J. Crank, G.S. Park (Eds.), Diffusion in Polymers, Academic Press, New York, 1968, p. 98.
[40] C. Giddings, Anal. Chem. 35 (1963) 1999.
[41] L. Fossey, F.F. Cantwell, Anal. Chem. 54 (1982) 1693.
[42] J. Wironen, C. Shen, J. Yan, C. Batich, J. Appl. Polym. Sci. 59 (1996) 825.
[43] S. May, R.A. Hux, F.F. Cantwell, Anal. Chem. 54 (1982) 1279.
[44] M.A. Jeannot, F.F. Cantwell, Anal. Chem. 68 (1996) 2236.
[45] P. Cornel, H. Sontheimer, R.S. Summers, P.V. Roberts, Chem. Eng. Sci. 41 (1986) 1801.
[46] P. Jandera, G. Guiochon, J. Chromatogr. 605 (1992) 1.
[47] S. Brunauer, L.S. Deming, W.E. Deming, E. Teller, J. Am. Chem. Soc. 62 (1940) 1723.
[48] F. Nevejans, M. Verzele, Chromatographia 20 (1985) 173.
[49] G.E. Boyd, A.W. Adamson, J.L.S. Myers, J. Am. Chem. Soc. 69 (1947) 2836.
[50] P.C. Hiemenz, Principles of Colloid and Surface Chemistry, Marcel Dekker, New York, 1986, Chapter 9.
[51] J.J. Kipling, Adsorption from Solutions of Non-Electrolytes, Academic Press, New York, 1965, Chapter 5.
[52] E.J. Simpson, R.K. Abukhadra, W.J. Koros, R.S. Schechter, Ind. Eng. Chem. Res. 32 (1993) 2269.
[53] D.M. Ruthven, Principles of Adsorption and Adsorption Processes, Wiley, New York, 1984, Chapters 5 and 6.
[54] S.J. Gregg, K.S.W. Sing, Adsorption, Surface Area and Porosity, Academic Press, New York, 1967, Chapter 3.
[55] F. Nevejans, M. Verzele, J. Chromatogr. 350 (1985) 145.
[56] J.M. O'Kane, D.N. Sherrington, Macromolecules 23 (1990) 5286.
[57] R. Arshady, Makromol. Chem. 189 (1988) 1295.
[58] J. Wironen, C. Shen, J. Yan, C. Batich, J. Appl. Polym. Sci. 59 (1996) 825.
[59] A.D. Wilks, D.J. Pietrzyk, Anal. Chem. 44 (1972) 676.
[60] Y. Jun, X. Rongnan, Y. Juntan, J. Appl. Polym. Sci. 38 (1989) 45.
[61] L.A. Errede, Polym. Preprints, Japan 26 (1985) 77.

[62] L.A. Errede, J. Appl. Polym. Sci. 31 (1986) 1749.
[63] L.A. Errede, J.D. Stoesz, L.M. Sirvio, J. Appl. Polym. Sci. 31 (1986) 2721.
[64] O. Okay, C. Gurun, J. Appl. Polym. Sci. 46 (1992) 421.
[65] L.R. Snyder, J. Chromatogr. 92 (1974) 223.
[66] J.C. Glajch, J.J. Kirkland, K.M. Squire, J.M. Minor, J. Chromatogr. 199 (1980) 57.
[67] Personal communication with D. Lee, Hamilton Co., September 1996.
[68] J.C. Giddings, Dynamics of Chromatography, Part I, Principles and Theory, Marcel Dekker, New York, 1965, Chapter 6.
[69] P. Meares, in: J. Crank, G.S. Park (Eds.), Diffusion in Polymers, Academic Press, New York, 1968, p. 373.
[70] T. Ohkuma, S. Hara, J. Chromatogr. 400 (1987) 47.
[71] L.R. Snyder, Principles of Adsorption Chromatography, Marcel Dekker, New York, 1968, Chapter 6.